JOURNAL OF MATERIALS SCIENCE 32 (1997) 1725–1731

Superconductivity and X-ray photoelectron spectroscopy studies of $Bi_2Sr_{2-x}La_xCaCu_2O_{8+\delta}$

C. NGUYEN-VAN-HUONG
Laboratoire de Physique du Solide, CNRS (UPR 05), ESPCI, 10 rue Vauquelin, 75231 Paris Cedex 05, France

C. HINNEN, J. M. SIFFRE
Laboratoire de Physico-Chimie des Surfaces, CNRS (URA 425), ENSCP, 11 rue Pierre et Marie Curie, 75231 Paris Cedex 05, France

The crystal structure (determined from X-ray diffraction measurements), the superconducting properties (from resistivity measurements) and electronic structure (from X-ray photoelectron spectroscopy investigation) of $Bi_2Sr_{2-x}La_xCaCu_2O_8$ compounds (substituted on the strontium site) have been studied for different lanthanum concentrations. A systematic increase in the lattice parameter *a* and a decrease in the *c*-axis with increasing x was observed. The ρ–T characteristics for different x showed that T_c increases up to 91 K ($x = 0.2$) then falls for higher doping, indicating that the substitution induces a decrease in the hole density. The superconductor–insulator transition occurred at a higher doping level ($x = 0.7$) than in the case of a substitution for calcium. This behaviour has been correlated to the change in the electronic structure. This was revealed by a lowering of the Fermi level and a shift towards lower energy of the core level X-ray photoelectron spectra Bi 4f. The different effect of the strontium substituted site in comparison with that of the calcium site has been tentatively explained by their respective crystallographic situations giving rise to different charge transfer and coupling between Bi–O and Cu–O_2 planes.

1. Introduction

It is now fairly well established that for high T_c superconductor (HTSC) cuprates, there is an optimum carrier concentration for the occurrence of superconductivity below which the material turns to the insulating state, while for larger concentration, it exhibits more metallicity. In this region, T_c can increase (underdoped range), pass through a maximum then decrease (overdoped range).

In general, the three types of behaviour (insulating, superconducting and metallic) can be brought about in a cuprate HTS by varying the carrier concentration. This can be performed either by oxygenation or by different cationic substitution at different sites. However, if the substituting cation is aliovalent with respect to the on-site cation, an ambiguity in the interpretation of the transport data may arise due to the change in the oxygen stoichiometry. In bismuth-based cuprate $Bi_2Sr_2CaCu_2O_8$, a large number of works used the effect of cationic substitution upon carrier concentration in order to determine the phase diagram of this compound. Most of the results were concerned with substituting for bismuth and calcium. For bismuth the substitution by lead leads to a change in the structural modulation (modification of the lattice parameters and increase of the modulation periodicity) and only a slight change in T_c [1–5]. The substitution for calcium by a rare-earth induces a large change in T_c with a metal–insulator transition for $0.5 < x < 0.6$ [6–11]. The observed effect was usually explained by the variation in the carrier concentration which should be considered as the result of both the aliovalent substitution and change in the oxygen stoichiometry. Few studies have reported the substitution for strontium, probably due to the difficulty of producing single-phase samples [12]. Koike *et al.* [13] have shown a variation of T_c and a metallic–insulator transition for $0.6 < x < 0.8$ by electrical and magnetic measurements. Up to now, no attempt has been made to explain this difference in the doping level for which the metal–insulator transition occurs.

In this work we have produced and studied single-phase $Bi_2Sr_{2-x}La_xCaCu_2O_{8+\delta}$ samples with varying doping levels ($0 \leqslant x \leqslant 1$). We chose La^{3+} because it most probably substitutes for Sr^{2+} in preference to Ca^{2+}, owing to the closer similarity of their ionic radii ($La^{3+} = 0.120$ nm, $Sr^{2+} = 0.128$ nm). The investigation was aimed at studying the influence of La^{3+} substitution for Sr^{2+} on the crystal structure, the superconducting properties (correlation between x and ρ and T_c) and the electronic structure determined by X-ray photoelectron spectroscopy (XPS). In the XPS studies we attempted to ensure that the

0022–2461

studied surfaces exhibited the properties of the bulk material [14, 15] and that the spectral changes reflected well the evolution of the material. The doping effect on the valence states of cations, structure of the valence band and position of the Fermi level were studied in detail.

2. Experimental procedure

A set of doped 2212 Bi compounds, $Bi_2Sr_{2-x}La_x$-$CaCu_2O_{8-\delta}$, with $0 \leqslant x \leqslant 1$ was studied. The samples were synthesized by the conventional solid-state reaction method with high-purity oxides Bi_2O_3, CuO, La_2O_3 and carbonates $SrCO_3$ and $CaCO_3$. The constituents were mixed, pelletized and fired in air successively at 810, 845 and finally 850 °C for 12 h each, with intermediate grindings for samples $x = 0$, 0.1 and 0.2, at 850, 870 and 900 °C for $x = 0.4$, 0.6 and 1. Finally, they were sintered for 22 h at 850 °C for $x = 0$, 880 °C for $x = 0.1$ and 0.2, and 900 °C for $x = 0.4$ and 0.6 and 1. The pellets were quenched to liquid nitrogen at the end.

The phases were characterized by powder X-ray diffraction (XRD) using a Philips automated X-ray diffractometer. The electrical resistivity was measured using a d.c. four-probe configuration. Electrical contacts for these measurements were made using silver paint fired at 400 °C for 1 h in flowing oxygen.

XPS measurements were taken with a VG ESCALAB MKII spectrometer using a non-monochromatized AlK_α source ($\hbar\nu = 1486.6$ eV). The spectrometer was calibrated with Au $4f_{7/2}$ at a binding energy (BE) of 83.8 ± 0.1 eV and with Cu $2p_{3/2}$ at BE $= 932.7 \pm 0.1$ eV. All the data were recorded at room temperature. Prior to XPS analysis, the ceramic sample surface was scraped and then immediately introduced into the preparation chamber where heating from room temperature to 200 °C under 10^{-5} mbar oxygen for 60 min was performed. We have checked, as in a previous paper [14], that such a treatment provided a surface exhibiting similar properties to the bulk.

The oxygen content was estimated by iodometric titration.

3. Results and discussion

3.1. Crystal structure

All the XRD patterns show well-defined peaks which are indexable on the basis of the tetragonal structure of Bi 2212 except for $x = 1$. Furthermore, there are no lines attributable to impurity phases, indicating that the samples are single-phase in agreement with that reported by Munakata *et al.* [6]. Fig. 1 shows the XRD patterns for $x = 0$, 0.4 and 1. The presence of second phase (2201) for $x = 0$ can be observed, in accordance with previous studies [16–18].

The deduced lattice parameters are plotted as a function of x in Fig. 2. As can be seen, there is a systematic increase in the lattice parameter a and decrease in the c-axis with increasing x. The decrease in the c-axis with increasing x is consistent with the substitution of smaller La^{3+} ($r = 0.120$ nm) for larger

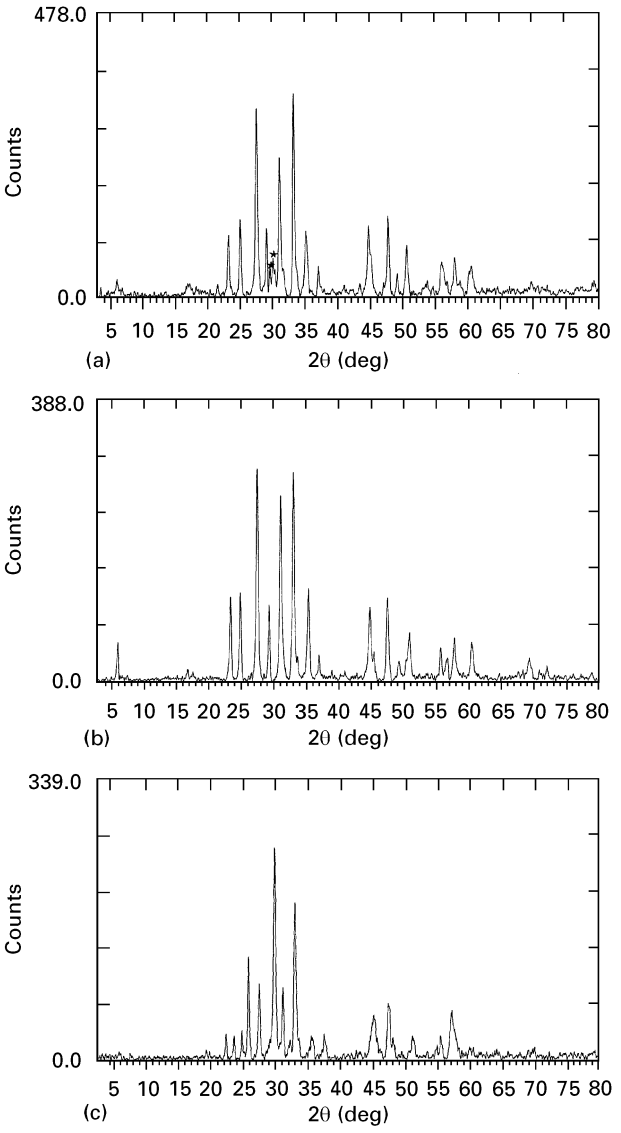

Figure 1 XRD patterns for $Bi_2Sr_{2-x}La_xCaCu_2O_8$ with $x =$ (a) 0, (b) 0.4 and (c) 1. (∗) Peaks attributed to 2201.

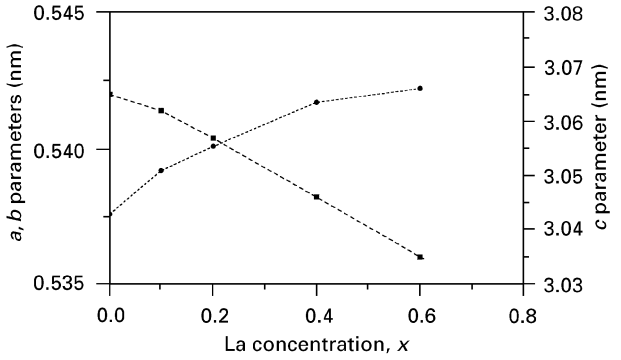

Figure 2 Lattice parameters (●) a, b and (■) c as a function of x for $Bi_2Sr_{2-x}La_xCaCu_2O_8$.

Sr^{2+} ($r = 0.128$ nm) ions. The increase in the a-axis with x is more complex. It could be attributed to the lengthening of the Cu–O bond in the $Cu–O_2$ planes, induced by electron doping brought about by substitution of divalent strontium by trivalent lanthanum, thus implying a decrease in the hole concentration in these planes.

3.2. Oxygen content

The substitution of divalent Sr^{2+} by trivalent La^{3+} is expected either to modify the copper valence or to bring into the structure some supplementary oxygen, or both, in order to maintain the charge neutrality. The oxygen content was determined by iodometric titration. Fig. 3 shows the evolution of the copper valency and the deduced oxygen content with doping. Whenever the oxygen content is not known directly, it can be reasonably considered that the evolution of these parameters with doping are significant. We note a continuous increase in the oxygen content and decrease in the copper valency with x varying from 0–1. The change in the oxygen content, δ, with doping is inferior to $x/2$ for all doping levels, leading to a diminution of copper valency with increasing x, but it still remains greater than 2 for $x = 1$ although it exhibits an insulating behaviour. This evolution in the copper valency has been confirmed by spectroscopic measurements, as described further.

3.3. Resistivity and critical temperature

The temperature dependence of the resistivity, ρ, for different x is shown in Fig. 4. For $0 \leqslant x \leqslant 0.4$, the material is metallic ($T > T_c$), and superconducting. For $x = 0.6$, it is still superconducting; the resistivity, however, shows a small semiconducting behaviour near to the superconducting transition. When $x = 1$, it is clearly an insulator. The metal–insulator transition

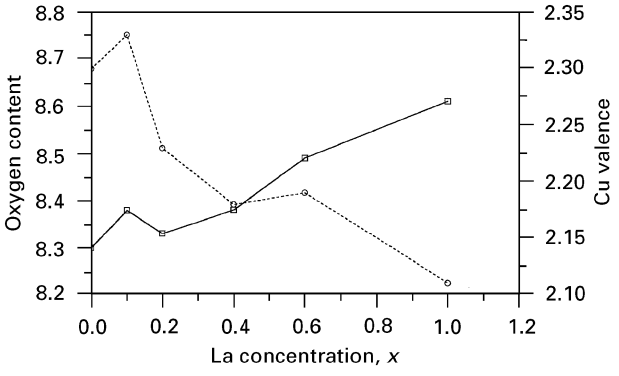

Figure 3 (□) Oxygen content and (○) copper valence as a function of x for $Bi_2Sr_{2-x}La_xCaCu_2O_8$.

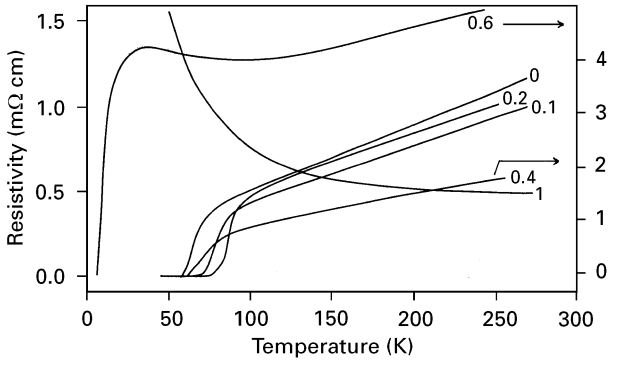

Figure 4 Resistivity transition for different lanthanum concentrations or $Bi_2Sr_{2-x}La_xCaCu_2O_8$.

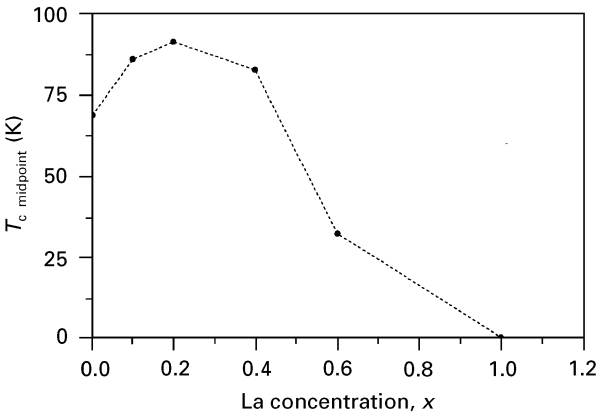

Figure 5 Critical temperature as a function of x for $Bi_2Sr_{2-x}La_x$-$CaCu_2O_8$.

was found to occur at the doping level between 0.7 and 1.

For $0 \leqslant x \leqslant 0.4$, the deviation from the equation $\rho = \rho_0 + \alpha T$, which expresses the metallic behaviour, occurs at a temperature increasing with x; this downward deviation may be attributed to the effect of thermal fluctuation.

Fig. 5 shows the dependence of transition temperature, $T_{c(midpoint)}$ with x. It can be seen that T_c increases up to 91 K for $x = 0.2$, then decreases for $x = 0.4$ and 0.6. These changes are likely related to the hole concentration in the $Cu–O_2$ plane. As each substitution of La^{3+} for Sr^{2+} fills one hole, a decrease is expected in the hole concentration on the $Cu–O_2$ planes. The observed increase in T_c for $0 < x$ 0.2 is consistent with the well-known fact that the system with $x = 0$ is overdoped. In that case Gupta and Gupta [19] have reported that the hole carrier density obtained by electronic structure calculation was 0.37 hole/$Cu–O_2$. As a substitution of 20% lanthanum for strontium raises the T_c of our samples from 70 K to 91 K, it appears that this substitution level likely brings the hole density to its optimum value (which is currently assumed to be 0.2–0.3 hole/$Cu–O_2$ unit). Similar trends were observed in substituting on the calcium site [9, 13, 20, 21].

The most remarkable fact is that for $x = 0.6$ the material remains superconducting and superconductivity disappears only for $x \geqslant 0.7$–0.8. When substituting for calcium, this metal–insulator transition occurs already for $x = 0.55$ [8, 13]. The superconductivity appears to be maintained at a higher substitution level for the strontium site. This can be tentatively explained by crystallographic and electrostatic considerations: the strontium site is closer to the apical oxygen of the $Cu–O_2$ plane and to the BiO plane than the calcium site. This geometric situation of the strontium site seems favourable to a charge compensation by the supplementary oxygen situated in the BiO plane. Moreover, the presence of La^{3+}, more charged than Sr^{2+}, in increasing the Coulomb interaction with neighbouring oxygen, thus shortens the Sr–O and $Cu–O_3$ (O_3 is the apical oxygen) bond lengths and induces a stronger coupling between Bi–O and $Cu–O_2$ planes than Sr^{2+} should do. This phenomenon may

compensate the hole filling and so maintain the superconductivity at a higher level than the substitution for Ca^{2+} does. This is consistent with the comparison of the c values observed for $x = 0.6$ and 1 for Sr^{2+} and Ca^{2+} substitution: c is lower for a substitution on the Sr^{2+} site than on the Ca^{2+} site.

A broadening of the resistive transition as a function of doping was observed as is seen in Fig. 4. This phenomenon has been described for similar compounds and differently interpreted. Tallon *et al.* [22] correlated this broad transition to intrinsic granularity, supported by the fact that the broad transition occurs only in the underdoped region. In contrast, Muroi and Street [23–25] explained in terms of phase inhomogeneity involving a percolative process between superconducting regions and insulating islands. Our observations may be more reasonably interpretated by the second model.

The normal-state resistivity measured at 250 K, ρ_n, as a function of doping is shown in Fig. 6. For $x \leqslant 0.2$ a slight decrease can be observed, for higher doping levels, ρ_n increases exponentially.

For $x = 1$, which showed a semiconducting behaviour, the resistivity could be fitted with the expression

$$\rho_T = \rho_0 \exp(T_0/T)^n \quad (1)$$

where T_0 and n are constants. The value of the exponent n determines the nature of the conduction mechanism [26]. A value of $n = 1/4$ corresponds to a three-dimensional variable-range-hopping (VRH) process and $n = 1/3$ to a two-dimensional VRH mechanism. As can be seen in Fig. 7 which represents the variation of log ρ as a function of $T^{-1/4}$ or $T^{-1/3}$, the difference between the two fittings is rather subtle. The fittings are fairly good in the low-temperature region. In the three-dimensional VRH process, the T_0 value is 1.4×10^4 K. Our T_0 value is of the same order of magnitude as those reported in the literature for substitution on the calcium site. Hopping conductivity in $Bi_2SrLaCaCu_2O_{8+\delta}$ implies that the electronic states are localized at the Fermi level by disorder, because La^{3+} has a different size, charge and electronic structure in comparison with strontium. Similar behaviour has been seen for other 2212 substituted systems $Bi_2Sr_2Ca_{1-x}Ln_xCu_2O_{8+\delta}$ where calcium was replaced by a lanthanide (Ln = Y, Ce or Ga, Pr and Gd) [27–29]. The substitution for strontium appears to induce the same type of perturbation.

3.4. XPS study

It is interesting to correlate the observed changes in superconducting properties with the change in electronic structure. Using X-ray photoelectron spectroscopy, we have studied how this chemical substitution affects the valence states of cations, structure of the valence band and position of the Fermi level.

After the *in situ* treatment, the survey XPS spectrum displayed the characteristic core levels of the elements constituting the material, and indicated a nearly complete absence of the C 1s peak; no other impurity peak was observed.

For pure 2212 and lead-doped 2212 [14], the O 1s spectra consisted of a main peak at 529.4 eV, assigned to oxygen bonded to cations; the small one at higher BE (531.2 eV) was assigned to remaining adsorbed H_2O and/or hydroxyl ions.

We analysed a series of samples with $x = 0$, 0.2, 0.6 and 1. For the sake of clarity, we report only the spectra corresponding to $x = 0$ and 1.

3.4.1. Valence band

The valence band spectra obtained for $x = 0$ and 1 are shown in Fig. 8. Only the spectrum for the insulating sample ($x = 1$) necessitated a correction from charging effect (0.3 eV). This charging effect was estimated by taking the spectra at different beam intensities (600 and 200 W). In the energy range -4 to 6 eV, the shape of the spectrum is similar to that previously observed for $Bi_2Sr_2CaCu_2O_{8+\delta}$ and $Bi_{1.6}Pb_{0.4}Sr_2CaCu_2O_{8+\delta'}$ [14]. For $x \leqslant 0.6$, a clear Fermi edge can be seen, indicating that the conductivity in the surface regions is metallic. In contrast, for $x = 1$, the intensity is low, as expected from the insulating character of the sample. The large valence band feature at about 3 eV is assigned to emission from bands derived from Cu–O hybrids ($Cu3d^9L$ or $Cu3d^9L^2$). As a whole, the shape is unchanged, only a shift to higher BE with doping is observed. The curves could be made to coincide with the others by shifting along the

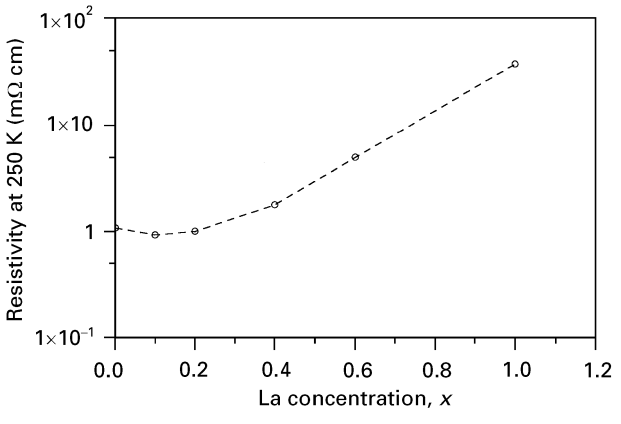

Figure 6 Variation of the normal-state resistivity measured at 250 K with doping x for $Bi_2Sr_{2-x}La_xCaCu_2O_8$.

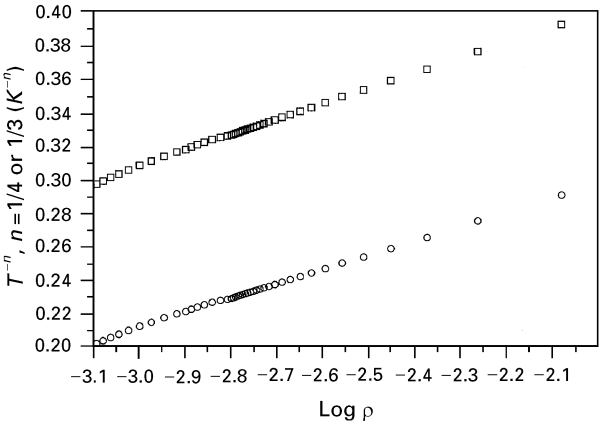

Figure 7 Variation of the logarithm of the resistivity with (□) $T^{-1/4}$ and (○) $T^{-1/3}$ for $x = 1$.

energy axis (0.1, 0.3 and 0.4 eV for $x = 0.2$, 0.6 and 1, respectively, see Table I). These shifts can be attributed to a lowering of the Fermi level, as a consequence of the expected (and observed above) decrease in the hole density. These values are comparable to those reported for $Bi_2Sr_2Ca_{1-x}Y_xCu_2O_{8+\delta}$ [9]. However, the shift is more important for the insulating sample in the case of substitution for Ca^{2+} than for Sr^{2+} (0.6 eV for $Bi_2Sr_2YCu_2O_{8+\delta}$ [9] and 0.4 for $Bi_2SrLaCaCu_2O_{8+\delta}$). This tends to show that for the same doping level ($x = 1$), the hole filling is lower for a substitution for Sr^{2+} than for Ca^{2+}.

It thus appears that the only influence of doping on the valence band spectrum obtained with XPS is a shift towards higher BE due to a change in E_F.

3.4.2. Core levels

In the following sections, all the binding energies were corrected from the change in the Fermi level.

Cu 2p. All the spectra are composed of a main component (Cu_{main}) associated with the $2p\ 3d^{10}L$ final state (L indicates a ligand hole) accompanied by a satellite (Cu_{Sat}) associated with the multiplet splitting of the $2p\ 3d^9$ final state at a higher energy of $\simeq 9$ eV. The Cu $2p_{3/2}$ core level XPS spectra corresponding to $x = 0$ and 1 are shown in Fig. 9. We characterized the Cu $2p_{3/2}$ spectra by the BE of the main peak, the full-width at half-maximum (FWHM) and the $I^{Cu}_{Sat}/I^{Cu}_{main}$ ratio. As can be seen in Table I, the BE of Cu_{main} and the FWHM remains unchanged with x, except for $x = 1$, which is characterized by a shift towards lower BE and a narrowing of the peak. The $I^{Cu}_{Sat}/I^{Cu}_{main}$ ratio increases with x up to $x = 0.6$ then decreases for $x = 1$. All these observations are consistent with a decrease in the formal valence of copper. The evolution in the $I^{Cu}_{Sat}/I^{Cu}_{main}$ ratio can be explained as follows [30]. With increasing x, the hole density decreases, the fraction of Cu^{2+}–O^{1-} decreases and the amount of Cu^{2+}–O^{2-} increases, leading to an increase in the satellite intensity (and the $I^{Cu}_{Sat}/I^{Cu}_{main}$ ratio) up to $x = 0.6$. For $x = 1$, the shift in the BE (0.3–0.4 eV), the noticeable narrowing of the main peak (2.8 instead of 3.4 eV) and the decrease in the $I^{Cu}_{Sat}/I^{Cu}_{main}$ prove the presence of some Cu^{1+}.

Bi 4f, La 3d, Sr 3d, Ca 2p. The data for the core levels of these elements are collected in Table II. As indicated, all the BE values were corrected from the change in E_F.

For $x = 0$, the Bi 4f core level spectrum is similar to that in Bi_2O_3: in the undoped sample, the valence of Bi is 3 +, as we have previously reported [14]. For doped samples (Fig. 10), the BE of Bi 4f shifts towards a lower energy, showing a decrease of the bismuth valency with doping. If we correlate the bismuth valence to a charge transfer process between Cu–O_2 and Bi–O planes, as suggested by Pham *et al.* [8] for undoped Bi 2212, our results show a transfer increase with doping and so are in contrast with their XAS results for $Bi_2Sr_2Ca_{1-x}Y_xCu_2O_{8+\delta}$. This observed increase in the charge transfer with x may explain why superconductivity is maintained at a higher doping level for $Bi_2Sr_{2-x}La_xCaCu_2O_{8+\delta}$ than for $Bi_2Sr_2Ca_{1-x}Y_xCu_2O_{8+\delta'}$.

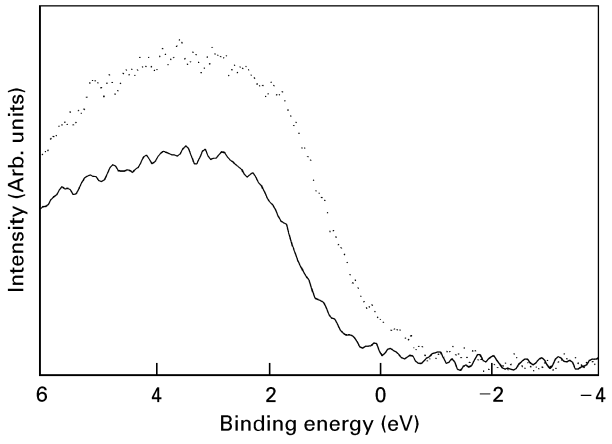

Figure 8 Valence band spectra of $Bi_2Sr_{2-x}La_xCaCu_2O_8$ in the -4 to 6 eV binding energy range for (----) $x = 0$ and (—) $x = 1$.

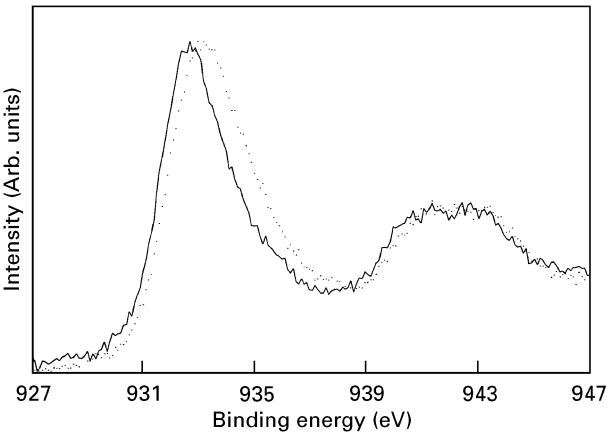

Figure 9 Cu $2p_{3/2}$ core level XPS spectra of $Bi_2Sr_{2-x}La_xCaCu_2O_8$ for (----) $x = 0$ and (—) $x = 1$ after correction for the charging effect and shift of the Fermi level.

TABLE I The Cu $2p_{3/2}$ XPS characteristics as a function of lanthanum concentration, x

x	Fermi level	Cu $2p_{3/2}$			
	ΔE_F (eV)	BE (eV)	BE corrected from ΔE_F (eV)	FWHM (eV)	$I^{Cu}_{Sat}/I^{Cu}_{main}$
0	0	933.1	933.1	3.4	0.33
0.2	0.1	933.2	933.1	3.4	0.40
0.6	0.3	933.3	933.0	3.2	0.42
1	0.4	933.1	932.7	2.8	0.37

TABLE II The Bi 4f, La 3d, Sr 3d and Ca 2p binding energies, corrected from the shift of the Fermi level, E_F, and charging effect, as a function of lanthanum concentration, x

x	Binding energy (eV)			
	Bi $4f_{7/2}$	La $3d_{5/2}$	Sr $3d_{5/2}$	Ca $2p_{3/2}$
0	158.4		131.9	345.2
0.2	158.2	833.8	131.9	345.3
0.6	158.0	833.8	131.9	345.4
1	157.8	833.7	131.9	345.7

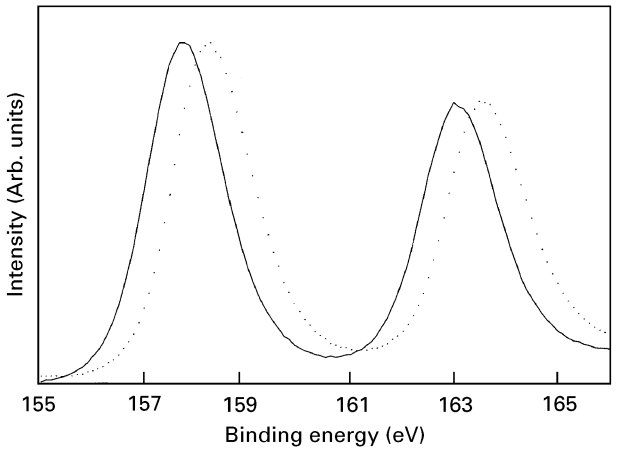

Figure 10 Bi 4f core level XPS spectra of $Bi_2Sr_{2-x}La_xCaCu_2O_8$ for (----) $x = 0$ and (—) $x = 1$ after correction for the charging effect and shift of the Fermi level.

While the Sr 3d core level remains unchanged, that of Ca 2p shifts significantly to higher BE with x. We have previously shown that the mixed occupancy of strontium and calcium was valid for BiPb 2212 [14], We have used here the same calculation procedure and deduced the occupation fractions and number of ions of strontium and calcium in the SrO and calcium layer. The obtained values are not noticeably different from the formal ones. Thus the shift in Ca 2p cannot be correlated to some occupation change but more probably to a change in the calcium valence. This shift was also observed in the case of substitution for calcium [7, 9–11] and attributed either to a change in the chemical environment, which considered changes in the valence state and bond length [9, 11], or to an increase in the calcium valence [7, 10].

The rare-earth compounds give rise to complex XPS line shapes. These line shapes are due to hybridization effects between the valence band of the solid and localized f states of rare-earth ions in the final state of photoionization. In the case of lanthanum, the photoionization of the 3d levels results in a situation in which the Coulomb attraction exerted by the core holes lowers the energy of $4f^1$ final state relative to the $4f^0$ final state to such an extent that both energies become comparable. This leads to a hybridization of the two states, giving rise to the typical two-peaked shape of the La 3d doublet components. This shape is observed in La_2O_3, in perovskite and in HTSC cuprates.

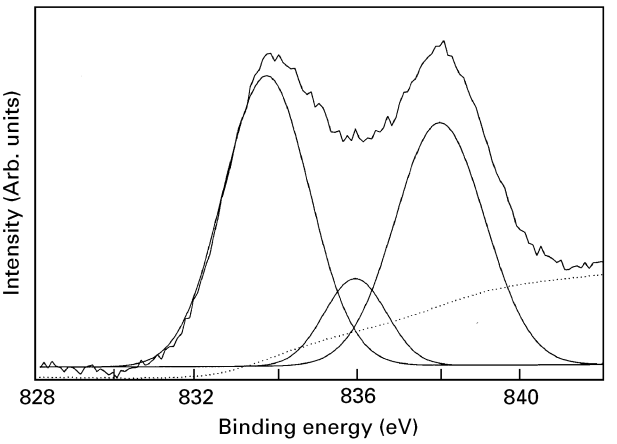

Figure 11 High-resolution XPS spectra of La $3d_{5/2}$ for $x = 1$ after correction for the charging effect and shift of the Fermi level.

In our sample, this type of spectrum was observed, as shown in Fig. 11, for $x = 1$. On the whole, the spectral lines are wider than those observed in La_2O_3 [31], in perovskite [32] or in zeolite [33] showing the influence of environment. The best fit of the spectrum in Fig. 11 was obtained with three components, two major peaks at BE = 833.6 and 837.9 eV, respectively, and a third small peak at an intermediate energy of 835.8 eV. These three components were valid to fit all the spectra relative to the different x, the most remarkable being the absence of the extra peak with increasing x. This shows that La^{3+} occupies a single site: that of Sr^{2+} as expected.

4. Conclusion

The present study has shown the influence of the substitution site Sr^{2+} or Ca^{2+} on some properties of Bi 2212 substituted compounds.

The phase diagram of Bi 2212 substituted compounds in which La^{3+} is substituted for Sr^{2+}, is analoguous to that reported for a substitution on the calcium site with a difference concerning the metallic–insulator transition. The transition occurs at a higher doping level for Sr^{2+} ($x \geqslant 0.7$) than for Ca^{2+} ($x \geqslant 0.5$) [8, 13]. We can explain this by the shortening of Sr–O and Cu–O_3 (O_3 is the apical oxygen) bond lengths leading to an increased coupling between Bi–O and Cu–O_2 planes favouring their charge transfer and thus superconductivity for a higher doping level. In the insulating regime, the conduction mechanism is of the three-dimensional variable range hopping type, implying the localization of state near the Fermi level.

A shift towards higher BE upon doping of the whole valence band is observed for both types of substitution. This shift was shown to be due to a lowering of the Fermi level induced by a decrease in the hole density. For $x = 1$, the lowering of the Fermi level of 0.4 eV measured for our Sr^{2+}-substituted compound is smaller than the value of 0.6 eV reported in the literature for a substitution on the calcium site [9]. This is consistent with the observed effect of the substituted site on the phase diagram. Furthermore, the

present XPS investigation provides proof of the existence of self-doping in these compounds, which increases with doping. This is revealed by the observed bismuth valency state change. The nearly unchanged lineshape of La $3d_{5/2}$ core level shows that lanthanum substitutes only for strontium as expected from the ionic radii. The change of Cu $2p_{3/2}$ lineshape (shift towards lower BE, narrowing of the main peak, decrease in the $I^{Cu}_{Sat}/I^{Cu}_{main}$ ratio) shows that the copper valency decreases with x, in agreement with results obtained by chemical titration.

References

1. N. FUKUSHIMA, H. NIU, S. NAKAMURA, S. TAKENO, M. HAYASHI and K. ANDO, *Physica C* **159** (1989) 777.
2. N. KNAUF, J. HARNISCHMACHER, R. BOROWSKI, B. RODEN and D. WOHLLEBEN, *ibid.* **173** (1991) 414.
3. M. BOEKHOLT, D. GÖTZ, H. IDINK, M. FLEUSTER, T. HAHN, E. WOERMANN and G. GUNTHERODT, *ibid.* **176** (1991) 420.
4. K. KOYAMA, S. KANNO and S. NOGUCHI, *Jpn J Appl. Phys.* **29** (1990) L 420.
5. S. KAMBE, T. MATSUOKA, M. KAWAI and M. TAKAHASHI, *Physica C* **1656** (1990) 25.
6. F. MUNAKATA, T. KAWANO, H. YAMAUCHI and Y. INOUE, *ibid.* **190** (1992) 471.
7. R. ITTI, F. MUNAKATA, K. IKEDA, Y. YAMAUCHI, N. KOSHIZUKA and S. TANAKA, *Phys. Rev. B* **43** (1991) 6249.
8. A. Q. PHAM, N. MERRIEN, A. MAIGNAN, F. STUDER, C. MICHEL and B. RAVEAU, *Physica C* **210** (1993) 350.
9. M. A. VAN VEENENDAAL, R. SCHLATMANN, G. A. SAWATZKY and W. A. GROEN, *Phys. Rev. B* **47** (1993) 446.
10. B. R. SEKHAR, P. SRIVASTAVA, N. L. SAINI, K. V. R. RAO- S. K. SHARMA, K. B. GARG, S. K. AGARWAL, V. P. S. AWANA and A. V. NARLIKAR, *Physica C* **206** (1993) 139.
11. Y. SHICHI, Y. INOUE, F. MUNAKATA and M. YAMANAKA, *Phys. Rev. B* **42** (1990) 939.
12. J. M. TARASCON, P. BARBOUX, G. W. HULL, R. RAMESH, L. H. GREENE, M. GIROUD, M. S. HEGDE and W. R. MCKINNON, *ibid.* **39** (1989) 4316.
13. Y. KOIKE, Y. IWABUCHI, S. HOSOYA, N. KOBAYASHI and T. FUKASE, *Phys. C* **159** (1989) 105.
14. C. HINNEN, C. NGUYEN VAN HUONG and P. MARCUS, *J. Electron Spectr. Rel. Phenom.* **73** (1995) 293.
15. R. P. VASQUEZ, *ibid.* **66** (1994) 209.
16. A. Q. PHAM, M. HERVIEU, A. MAIGNAN, C. MICHEL, J. PROVOST and B. RAVEAU, *Phys. C* **194** (1992) 243.
17. G. S. GRADER, E. M. GYORGY, P. R. GALLAGHER, H. M. O'BRYAN, D. W. JOHNSON JR, S. SUNSHINE, S. M. ZALHUIRAK, S. JIN and R. S. SHERWOOD, *Phys. Rev. B* **38** (1988) 747.
18. J. M. TARASCON, Y.LE PAGE, P. BARBOUX, B. G. BAGLEY, L. H. GREENE, W. R. MCKINNON, G. W. HULL, M. GIROUD and D. M. HWANG, *ibid.* **37** (1988) 9382.
19. R. P. GUPTA and M. GUPTA, *ibid.* **49** (1994) 13154.
20. A. FUJIKAMI, R. YOSHIZAKI, M. AKAMATSU, T. ISHIGAKI and H. ASANO, *Phys. C* **174** (1991) 359.
21. F. JORDAN, O. PENA and R. HORYN, *ibid.* **235–240** (1994) 945.
22. J. L. TALLON, R. G. BUCKLEY, E. M. HAINES, M. R. PRESLAND, A. MAWSLEY, N. E. FLOWER and J. LORAM, *ibid.* **185–189** (1991) 855.
23. M. MUROI and R. STREET, *ibid.* **246** (1995) 357.
24. *Idem*, *ibid.* **208** (1993) 107.
25. M. MUROI and R. STREET, *Physica C* **216** (1993) 345.
26. N. F. MOTT, *J. Non Cryst. Solids* **1** (1969) 1.
27. R. K. NKUM and W. R. DATARS, *Phys. Rev. B* **46** (1992) 5686.
28. V. P. S. AWANA, S. K. AGARWAL, A. V. NARLIKAR and M. P. DAS, *Phys. Rev. B* **48** (1993) 1211.
29. Y. GAO, P. PERNAMBUCO-WISE, J. E. CROW, J. O'REILLEY, N. SPENCER, H. CHEN and E. SALOMON, *ibid.* **45** (1992) 7436.
30. C. S. GOPINATH, S. SUBRAMANIAN, P. SUMANA PRABHU, M. S. RAMACHANDRA RAO and G. V. SUBBA RAO, *Physica C* **218** (1993) 117.
31. C. D. WAGNER, W. M. RIGGS, L. E. DAVIS, J. F. MOULDER and G. E. MUILENBERG, "Handbook of XPS" (Perkin-Elmer, Minneapolis, 1979) 1996.
32. M. C. PRADIER and C. HINNEN, private communication.
33. W. GRÜNERT, U. SAUERLANDT, R. SCHLÖGL and H. G. KARGE, *J. Phys. Chem.* **97** (1993) 1413.

Received 19 April
and accepted 17 September 1996